Available states and available space: static properties that predict self-diffusivity of confined fluids

Gaurav Goel[1]**, William P Krekelberg**[1]**, Mark J Pond**[1]**, Jeetain Mittal**[2]**, Vincent K Shen**[3]**, Jeffrey R Errington**[4] **and Thomas M Truskett**[1,5]

[1] Department of Chemical Engineering, The University of Texas at Austin, Austin, TX 78712, USA
[2] Laboratory of Chemical Physics, National Institute of Diabetes and Digestive and Kidney Diseases, National Institutes of Health, Bethesda, MD 20892-0520, USA
[3] Chemical and Biochemical Reference Data Division, NIST, Gaithersburg, MD 20899-8320, USA
[4] Department of Chemical and Biological Engineering, University at Buffalo, The State University of New York, Buffalo, NY 14260, USA
[5] Institute for Theoretical Chemistry, The University of Texas at Austin, Austin, TX 78712, USA
E-mail: goel@che.utexas.edu, krekel@che.utexas.edu, mjp736@che.utexas.edu, jeetain@helix.nih.gov, vincent.shen@nist.gov, jerring@buffalo.edu and truskett@che.utexas.edu

Abstract. Although classical density functional theory provides reliable predictions for the static properties of simple equilibrium fluids under confinement, a theory of comparative accuracy for the transport coefficients has yet to emerge. Nonetheless, there is evidence that knowledge of how confinement modifies static behavior can aid in forecasting dynamics. Specifically, recent molecular simulation studies have shown that the relationship between excess entropy and self-diffusivity of a bulk equilibrium fluid changes only modestly when the fluid is isothermally confined, indicating that knowledge of the former might allow semi-quantitative predictions of the latter. Do other static measures, such as those that characterize free or available volume, also strongly correlate with single-particle dynamics of confined fluids? Here, we

investigate this question for both the single-component hard-sphere fluid and hard-sphere mixtures. Specifically, we use molecular simulations and fundamental measure theory to study these systems at approximately 10^3 equilibrium state points. We examine three different confining geometries (slit pore, square channel, and cylindrical pore) and the effects of particle packing fraction and particle–boundary interactions. Although average density fails to predict some key qualitative trends for the self-diffusivity of confined fluids, we provide strong empirical evidence that a new generalized measure of available volume for inhomogeneous fluids correlates excellently with self-diffusivity across a wide parameter space in these systems, approximately independently of the degree of confinement. An important consequence, which we demonstrate here, is that density functional theory predictions of this static property can be used together with knowledge of bulk fluid behavior to semi-quantitatively estimate the self-diffusion coefficient of confined fluids under equilibrium conditions.

Contents

1. Introduction

Confining an equilibrium fluid of particles to length scales on the order of several particle diameters changes both its static and dynamic properties. Classical density functional theory (DFT) can often make reliable predictions concerning the former, but implications of confinement for dynamics remain challenging to forecast for even the most basic models. For example, Enskog theory generalized for inhomogeneous fluids [1]

predicts that constant-activity confinement of the hard-sphere (HS) fluid between hard walls will significantly decrease self-diffusivity parallel to the boundaries [2]. Recent molecular dynamics simulations of that system, however, show that this prediction is qualitatively incorrect, i.e., self-diffusivity increases with constant-activity confinement [3]. Hydrodynamic theories, on the other hand, can predict how the presence of a single wall [4] or confinement between two walls [5]–[8] impacts the self-diffusion of a single Brownian particle in solvent. But it is not yet clear how to generalize these approaches to account for the effects that strongly inhomogeneous static structuring has on the transport coefficients of dense confined fluids [3, 9, 10]. Given the absence of a reliable microscopic theory, the development of new qualitative or semi-quantitative heuristics for predicting dynamics of confined fluids would be of considerable practical use.

In this spirit, one productive strategy has been to first exhaustively simulate the static and dynamic behaviors of simple models of confined fluids. The idea is that comprehensive study of these systems may reveal static quantities that strongly correlate with transport coefficients for a wide variety of confining environments. Knowledge of these correlations together with reliable predictions of the static quantities from equilibrium theory would, in turn, lead to indirect predictions for how confinement modifies dynamics.

Indeed, recent simulation data covering hundreds of state points for various confined HS, Lennard-Jones, and square well fluids point to the existence of a robust, isothermal correlation between the self-diffusion coefficient D and the excess entropy per particle (over ideal gas) s^{ex}—a relationship that is approximately independent of the degree of confinement for a wide range of equilibrium conditions [3, 9], [11]–[13]. The practical implication is that the mathematical form of the correlation for a given fluid (obtained from bulk fluid simulations) can be used together with knowledge of the excess entropy of the confined system (computed, e.g., via DFT) to make a heuristic estimate for how confinement will modify the self-diffusivity. As has been discussed elsewhere [3, 9], this strategy can successfully predict subtle, confinement induced effects of packing frustration on relaxation processes, behavior not reflected in other static quantities traditionally thought to track dynamics, such as the average density.

Although a fundamental and general derivation that explains the observed relationship between excess entropy and dynamics of confined fluids is still lacking, the fact that the two are connected is not surprising. Excess entropy is a negative quantity that measures the extent to which static interparticle correlations reduce the number of microstates available to the fluid. In fact, $-s^{\mathrm{ex}}$ is often used as a metric for characterizing the 'amount' of structural order present in condensed phase systems [14]–[18]. Since interparticle correlations strongly influence collisional processes, it makes intuitive sense that macrostate changes which increase structural order $(-s^{\mathrm{ex}})$ might also tend to reduce single-particle mobility. Qualitative arguments such as these have previously been presented to rationalize empirically observed correlations between excess entropy and transport coefficients of both bulk [19]–[21] and confined [3], [9]–[13] equilibrium fluids. Nonetheless, it is natural to wonder whether excess entropy is unique in this regard. Perhaps other measures also accurately forecast the implications of confinement for the dynamics of dense fluids. For example, does the mobility of inhomogeneous HS fluids also increase with the average amount of space available for particle motion? Do some measures of free or available volume correlate much more strongly with dynamics than others? Can one quantitatively, or semi-quantitatively, predict self-diffusivity of confined

fluids on the basis of knowledge of how confinement affects the free or available volume of the system?

Here, we put the above questions to stringent tests for a variety of confined fluid systems. To ascertain the effect of pore geometry on correlations between self-diffusivity and thermodynamics, we study a monodisperse hard-sphere fluid confined to smooth hard-wall slit pores, square channels, and cylindrical pores. We also explore the effects of boundary interactions in the slit pore geometry by examining cases for which square well (attractive) or square shoulder (repulsive) particle–boundary interactions are present. Finally, we investigate the self-diffusivity and thermodynamics of a confined binary hard-sphere mixture which can be equilibrated in the fluid state at higher packing fractions without crystallizing than the corresponding single-component fluid. Altogether, this study represents, to our knowledge, the most comprehensive exploration of the relationships between self-diffusivity and static properties in these basic inhomogeneous systems to date. We calculate the self-diffusion coefficient (via molecular dynamics simulations), and excess entropy and various measures of available volume (via transition matrix Monte Carlo (TMMC) simulations and fundamental measure theory) at approximately 10^3 state points. Our results illustrate that accurate theoretical predictions of either excess entropy or a generalized measure of average available volume from classical density functional theory can be used together with knowledge of bulk fluid behavior to heuristically estimate the diffusion coefficient of confined fluids across a wide range of equilibrium conditions.

2. Connections between density, available volume, and dynamics: preliminary evidence

The available volume in a configuration of the single-component HS fluid refers to the space into which the center of an additional HS particle of equal size can be inserted without creating an overlap with existing particles or the boundary. It might also be considered a coarse measure of the space immediately available for particle motion in that configuration of the system. For the bulk equilibrium HS fluid, the ensemble averaged fraction of the total volume that is available (in the above sense) is given by $p_0 = \rho/\xi$ [22], where ρ is number density, $\xi = \exp[\beta\mu]/\Lambda^3$ is activity, μ is the chemical potential, $\beta = [k_B T]^{-1}$, k_B is the Boltzmann constant, T is the temperature, and Λ is the thermal de Broglie wavelength. It is known that increasing ρ monotonically decreases both p_0 and self-diffusivity D for this system; i.e. $\mathrm{d}p_0/\mathrm{d}\rho < 0$ and $\mathrm{d}D/\mathrm{d}\rho < 0$ (see, e.g., [18]), which is consistent with the intuitive idea that these static and dynamic properties might be linked. In the low particle density limit, some analytical results relating transport coefficients to static properties are also known. For example, Rosenfeld has used kinetic theory together with a second-virial expansion of thermodynamic properties to show that self-diffusivity, viscosity, and thermal conductivity of hard- and soft-sphere fluids scale in a simple way with s^{ex} [20]. The same line of reasoning predicts an analytical low density scaling between D and p_0 for this class of systems.

Are density, available space, and self-diffusion connected in the same qualitative way for inhomogeneous HS fluids? Previous studies have provided some information useful for addressing this question. For example, it is known that confining the equilibrium HS fluid between hard walls (while maintaining fixed ξ) significantly increases the average particle density, i.e. $(\partial\rho_{\mathrm{h}}/\partial h^{-1})_\xi > 0$, over a wide range of ρ_{h} and h [2, 3]. Here, $\rho_{\mathrm{h}} = N/(Ah)$ is
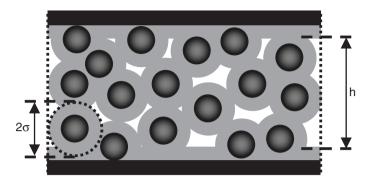
Figure 1. Schematic of an inhomogeneous HS fluid confined between boundaries in a slit pore geometry. The walls are placed a distance $H = h + \sigma$ apart, where h is the length accessible to particle centers. Dark regions indicate hard spheres and confining walls. Additional particle centers are excluded from the gray (overlap) region. The white region indicates the volume available for inserting an identical hard sphere of diameter σ.

average density, N is the total number of particles, A is the area of the interface between the fluid and one hard wall, and h is the center-accessible width of the slit pore (i.e., not including the 'dead space' that the particle centers are excluded from due to their interaction with the boundaries (see figure 1)). The fact that ρ_h increases upon constant-ξ confinement initially appeared consistent with earlier kinetic theory predictions that D of this system would show a corresponding decrease [2]. However, recent simulation data have demonstrated that the kinetic theory predictions were qualitatively incorrect [3]. That is, both ρ_h and D typically increase upon constant-ξ confinement $((\partial D/\partial\rho_h)_\xi > 0$, the fluid gets 'denser' on average and particles diffuse *more rapidly*), a trend that is the opposite of what might be expected on the basis of the bulk HS fluid behavior. Interestingly, confined HS fluids show a different trend when an alternative thermodynamic constraint is applied. Specifically, if h is held fixed, then increasing ρ_h has the effect of *decreasing D*, i.e., $(\partial D/\partial\rho_h)_h < 0$ [3, 11]. This preliminary information illustrates that knowledge of how ρ_h changes is not, in and of itself, enough for even qualitatively predicting the implications of confinement for the dynamics of a fluid. Indeed, in section 4 of this paper, we present extensive numerical evidence for a variety of confined fluid systems which underscores this point. We also explore whether adopting a definition of average density based on the total rather than center-accessible volume of the pore (see also [3, 11]) improves predictions for how confinement modifies dynamics.

Does available volume show a more reliable correlation to dynamics than average density? The fractional available volume in an inhomogeneous fluid is inherently a local quantity, and it is given by $p_{0i}(z) = \rho_i(z)\exp[\beta u_i^w(z)]/\xi_i$, where $\rho_i(z)$ and $u_i^w(z)$ represent the singlet (one-particle) density and the wall–particle interaction potential for species i, respectively, evaluated at a distance z from one wall [23]–[25]. The volume averaged quantity can be expressed as

$$\overline{p_{0i}} \equiv \frac{1}{V_{c,i}} \int_{V_{c,i}} p_{0i}\, \mathrm{d}V \qquad (1)$$

where the integral is over the particle-center-accessible volume $V_{c,i}$. For the special case of a single-component HS fluid confined between smooth hard walls, equation (1) reduces to

$\overline{p_0} = \rho_h/\xi$. Note that since $(\partial\overline{p_0}/\partial h^{-1})_\xi = \xi^{-1}(\partial\rho_h/\partial h^{-1})_\xi$, and $(\partial\rho_h/\partial h^{-1})_\xi > 0$ across a wide range of ρ_h and h [2, 3], it follows that $(\partial\overline{p_0}/\partial h^{-1})_\xi > 0$ for those conditions. This increase in the fraction of available space with constant-ξ confinement provides a simple physical explanation for the counterintuitive observation that D *increases* along the same thermodynamic path. The density-dependent behavior of the $\overline{p_0}$ under the constraint of constant h is also qualitatively consistent with the dynamical trends of the confined HS fluid. In particular, both $(\partial\overline{p_0}/\partial\rho_h)_h < 0$ and $(\partial D/\partial\rho_h)_h < 0$. All of this strongly suggests that $\overline{p_0}$ is a more relevant static metric for particle mobility than the average particle density ρ_h.

In the following sections, we test the generality of these preliminary observations by carrying out an extensive quantitative comparison of the correlations between self-diffusivity D and various static measures (density, excess entropy, and fractional available space) for single-component and binary HS fluids confined to a variety of channels with different geometries and particle–boundary interactions. The results clarify which of these static quantities reliably predict the implications of confinement for the self-diffusivity of the fluid particles.

3. Methods

We study single-component HS fluids of particles with diameter σ both in the bulk and confined to channels with three kinds of geometries: (i) quasi-two-dimensional slit pores, (ii) quasi-one-dimensional square channels, and (iii) cylindrical pores. Specifically, we consider (i) seven slit pores with thickness $H/\sigma = 5, 6, 7, 8, 9, 10$ and 15 in the confining z direction (see figure 1) together with periodic boundary conditions in the x and y directions, (ii) seven square channels with total x–y cross-sectional dimensions of $H^2/\sigma^2 = 25, 36, 49, 64, 81, 100$ and 225 together with a periodic boundary condition in the z direction, and (iii) six cylindrical channels of total diameter $H/\sigma = 6, 7, 8, 9, 10$ and 15 together with a periodic boundary condition in the axial z direction.

We take the interaction of a particle with a channel wall $u_w(s)$ in all cases to have a generic square well form:

$$u_{\mathrm{SW}}(s) = \begin{cases} \infty & s < \sigma/2 \\ \epsilon_w & \sigma/2 \le s < \sigma \\ 0 & s \ge \sigma \end{cases} \qquad (2)$$

where s is the shortest distance between the particle center and the wall of interest. For all three geometries, we study the case $\epsilon_w = 0$, i.e. smooth hard boundaries. Additionally, for the slit pore with size $H/\sigma = 5$, we investigate cases with $\epsilon_w = 2k_BT$ (a repulsive shoulder) and $\epsilon_w = -2k_BT$ (an attractive well).

We also consider a binary HS mixture confined between smooth hard walls in a slit pore of width $H/\sigma_1 = 5$. For this system, the particle diameter ratio is taken to be $\sigma_2/\sigma_1 = 1.3$ and the particle masses are proportional to their volume, i.e., $m_2/m_1 = (\sigma_2/\sigma_1)^3$. These parameter values closely mimic those examined in recent experiments of binary colloidal mixtures under confinement [26].

To explore dynamic properties of these fluids, we perform molecular dynamics simulations using an event-driven algorithm [27] in the microcanonical ensemble with $N = 4000$ particles for monodisperse HS systems and $N = 3200$ for the binary HS

systems. For bulk systems, we use a cubic simulation cell of volume V. For the confined systems, we adopt a rectangular parallelepiped simulation cell of volume $V = H_x H_y H_z$ with appropriate boundary conditions depending on geometry. We extract the self-diffusivity D by fitting the long-time ($t \gg \sigma_1 \sqrt{m_1 \beta}$) mean squared displacement to the Einstein relation $\langle \Delta \mathbf{r}_{d_p}^2 \rangle = 2 d_p D t$, where $\langle \Delta \mathbf{r}_{d_p}^2 \rangle$ corresponds to motions in the d_p periodic directions. For the sake of clarity, we reserve the symbol D for the self-diffusivity of fluids under confinement and D_{bulk} for the self-diffusivity of the bulk fluid. To obtain reliable estimates, we average self-diffusivities over four independent trajectories. For simplification, we report quantities from this point forward implicitly non-dimensionalized by appropriate combinations of the characteristic length scale, taken to be the HS diameter of the smallest particle in the fluid σ_1, and a characteristic timescale, given by $\sigma_1 \sqrt{m_1 \beta}$. Thus, all energies are implicitly per unit $k_B T$, and T is effectively scaled out of the problem altogether.

We obtain thermodynamic properties using grand canonical transition matrix Monte Carlo (GC-TMMC) simulation. For pure fluids, we use an algorithm presented by Errington [28] and for binary mixtures we employ a strategy developed by Shen and Errington [29], wherein one combines a series of semigrand ensemble simulations to construct the system's free energy over a wide range of densities and compositions. We conduct GC-TMMC simulations in a standard grand canonical ensemble where the volume V, temperature T, and activities $\{\xi_1, \xi_2\}$ are held constant and the particle numbers $\{N_1, N_2\}$ and energy E fluctuate. For notational convenience, we denote the sets $\{N_1, N_2\}$ and $\{\xi_1, \xi_2\}$ as $\mathbf{N}$ and $\boldsymbol{\xi}$, respectively, using conventional vector notation. The activity of component i is defined as $\xi_i = \Lambda_i^{-3} \exp(\mu_i)$, where μ_i is the chemical potential and Λ_i is the thermal de Broglie wavelength. For the pure component GC-TMMC simulations that we present here, we set $\xi = 1$ and adjust the particle-center-accessible volume V_c to make the total volume $V \approx 1000$. Simulations of the binary mixture use $V = 125$ and 245 for the bulk and confined fluids, respectively. For the bulk and confined simulations, we set $\xi_1 = 173.7$ and $\xi_2 = 381.5$.

The key quantity that we extract from the GC-TMMC simulations is the particle number probability distribution $\Pi(\mathbf{N})$. Once we obtain this distribution, we use basic statistical mechanics principles and histogram reweighting [30] to evaluate thermophysical properties over a range of activity values. First, we use histogram reweighting to deduce $\Pi(\mathbf{N})$ at a set of activities $\boldsymbol{\xi}_{\text{new}}$ generally different from that of the GC-TMMC simulation $\boldsymbol{\xi}_{\text{sim}}$,

$$\ln \Pi(\mathbf{N}; \boldsymbol{\xi}_{\text{new}}) = \ln \Pi(\mathbf{N}; \boldsymbol{\xi}_{\text{sim}}) + \sum_i N_i (\ln \xi_{i,\text{new}} - \ln \xi_{i,\text{sim}}) \tag{3}$$

where it is understood that the probability distributions are not normalized. We obtain average particle numbers $\langle \mathbf{N} \rangle$ from first-order moments of $\Pi(\mathbf{N})$,

$$\langle \mathbf{N}(\boldsymbol{\xi}) \rangle = \sum \mathbf{N} \Pi(\mathbf{N}; \boldsymbol{\xi}) \Big/ \sum \Pi(\mathbf{N}; \boldsymbol{\xi}). \tag{4}$$

We calculate ρ and ρ_h via normalization of $\langle \mathbf{N} \rangle$ by V and V_c, respectively.

We define excess entropy as the difference between the fluid's entropy and that of an ideal gas with the same density profile. The particle number probability distribution provides the density and composition dependence of the Helmholtz free energy at a given temperature. Therefore, we combine knowledge of $\Pi(\mathbf{N})$, average excess configurational

energies $U^{\mathrm{ex}}(\mathbf{N})$, and particle-number-specific spatial density distributions $\rho(\mathbf{N}, \mathbf{r})$ to obtain the total excess entropy S^{ex} [11, 13, 16],

$$S^{\mathrm{ex}}(\mathbf{N}) = U^{\mathrm{ex}}(\mathbf{N}) + \ln \Pi(\mathbf{N})/\Pi(\mathbf{0})$$
$$+ \sum_i \left\{ \ln N_i! - N_i \ln \xi_i - N_i \ln N_i + \int \rho_i(\mathbf{N}, \mathbf{r}) \ln \rho_i(\mathbf{N}, \mathbf{r}) \, \mathrm{d}\mathbf{r} \right\}. \qquad (5)$$

We also predict the thermodynamic quantities of the bulk single-component and binary HS fluids using the Carnahan–Starling [31] and Boublik–Mansoori–Carnahan–Starling–Leland [32, 33] equations of state, respectively. We predict the thermodynamic properties of confined HS fluids using a recent modification [34, 35] of Rosenfeld's fundamental measure theory [36]. Fundamental measure theory is a classical DFT of inhomogeneous fluids that has been shown to accurately predict structure and thermodynamics of confined HS systems in various restrictive geometries up to very high densities [37]. For numerical evaluation of the DFT for slit and cylindrical pores, we use Picard iterations on a grid spacing of 0.005. We update densities according to $[\rho]_{n+1}^{\mathrm{in}} = 0.95[\rho]_n^{\mathrm{in}} + 0.05[\rho]_n^{\mathrm{out}}$, where $[\rho]_{n+1}^{\mathrm{in}}$ and $[\rho]_n^{\mathrm{in}}$ are the input density profiles at the $(n+1)$th and nth iterations, respectively, and $[\rho]_n^{\mathrm{out}}$ is the output density profile at the nth iteration. We stop Picard iterations when the relative change in output density profile between two successive cycles (1 cycle = 20 iterations) becomes less than 10^{-5}. For numerical evaluation of the DFT in the square channel geometry, we use the Sandia National Laboratories Tramonto package [38]. We adopt a grid of 0.05×0.05 for $H = 5, 6$ and a grid of 0.075×0.075 for $H > 6$. We stop the minimization algorithm when the relative or absolute change in the grand potential is less than 10^{-7}.

4. Testing structure–property relations for predicting self-diffusivity of confined fluids

In this section, we explore the accuracy of the following strategy for predicting the self-diffusivity of confined HS fluids: (1) determine the value of a static quantity x of a confined fluid believed to be relevant for dynamics (e.g., its density, excess entropy, or fractional available volume), and (2) input this value into the relationship between self-diffusivity and that same static quantity for the bulk fluid, $D_{\mathrm{bulk}}^x(x)$, to estimate the confined fluid self-diffusivity, D. Of course, such a strategy can only provide approximate predictions. While there is a one-to-one relationship for the equilibrium HS fluid between the self-diffusivity and any one of the aforementioned static quantities[6], the dynamic properties of the confined fluid generally depend on a larger number of variables (e.g., the dimensions of the confining geometry, the nature of the particle–boundary interactions, and the chemical potential). Nonetheless, the hope is that one can discover a static quantity x whose relationship with D is largely insensitive to the effect of confinement. If so, the bulk structure–property relationship D_{bulk}^x can be used to predict D independently of the other parameters of the confined system. Systematic tests of this idea should give new insights into the structural properties that are most relevant for single-particle dynamics of inhomogeneous fluids.

---

[6] This is true if the self-diffusivity is appropriately non-dimensionalized, as it is here, to remove the trivial effect of the thermal velocity of the particles.

To investigate the accuracy of predictions by this approach, we use the 'exact' results of molecular simulations to examine the ratio of the bulk fluid self-diffusivity to that of confined fluids with the same value of x, i.e., D_{bulk}^x/D. Since one is often interested in both D and the effective characteristic time associated with diffusive motion (D^{-1}), we present plots of D_{bulk}^x/D in this work on a logarithmic scale, a representation for which overpredictions and underpredictions of D by the same factor appear the same distance from unity. We also present statistics associated with the relative errors of the predictions for different x. For each x that we consider here, we analyze roughly 10^3 state points of the equilibrium HS fluid confined to the various pore geometries described in section 3. This data set, when taken as whole, spans approximately four decades in D.

4.1. Confinement in channels with smooth hard boundaries

Here, we examine the ratio D_{bulk}^x/D for the single-component HS fluid confined to various geometries by smooth hard boundaries (i.e. $\epsilon_{\mathrm{w}} = 0$; see (2)). We begin by testing the predictions that follow from assuming that $x = \rho_{\mathrm{h}}$, the number density averaged over the particle-center-accessible volume of the pore, is the relevant static metric for dynamics (see figures 2(a)–(c)). It is immediately clear from the data that ρ_{h} does not, in itself, provide a good basis for prediction. HS fluids confined in slit pore, square channel, and cylindrical geometries generally exhibit a wide range of D for each ρ_{h}, with the fastest dynamics occurring in the smallest pores. In fact, note that the bulk structure–property relation $D_{\mathrm{bulk}}^{\rho_{\mathrm{h}}}$ can underpredict D by nearly a factor of ten for fluids in the most restrictive geometries. The performance of the bulk structure–property relation using $x = \rho_{\mathrm{h}}$ is actually even worse than it appears in figures 2(a)–(c) for the following reason. The freezing transition occurs at a density of 0.945 for the bulk HS fluid, which provides an upper limit on values of ρ_{h} that can be used for predictions using $D_{\mathrm{bulk}}^{\rho_{\mathrm{h}}}$. However, center-accessible densities for the equilibrium fluid in the smallest square channel and cylindrical pores can reach as high as $\rho_{\mathrm{h}} \approx 1.25$. Thus, the bulk structure–property relation $D_{\mathrm{bulk}}^{\rho_{\mathrm{h}}}$ *cannot even make predictions* for a significant fraction of the equilibrium state points for highly confined HS fluids. All of this confirms the preliminary expectation discussed in section 2 that knowledge of ρ_{h} and bulk fluid behavior is not enough for predicting the self-diffusivity of confined fluids. This conclusion is consistent with the earlier observations of Mittal *et al* [11] concerning a smaller set of data for the HS fluid confined to slit pores.

In figures 2(d), (g) and (j), we again present D_{bulk}^x/D for the HS fluid confined to slit pores, but now D_{bulk}^x is the corresponding bulk fluid relation between diffusivity and one of three alternative static properties (x): average density based on total pore volume $\rho = \rho_{\mathrm{h}}(1 - H^{-1})$, excess entropy per particle s^{ex}, and fraction of available volume $\overline{p_0}$. The data in these plots correspond to confined fluid states with packing fractions that vary from the dilute gas to the freezing transition for pore widths $H \geq 5$. As can be seen, each of these static measures can provide semi-quantitative predictions for confined fluid diffusivities when used together with the corresponding bulk structure–property correlation. In fact, for 93% ($x = \rho$), 97% ($x = s^{\mathrm{ex}}$), and 100% ($x = \overline{p_0}$) of equilibrium state points for these systems, the predictions provided by D_{bulk}^x are within 20% of the 'exact' MD data for D. Note that the very small fraction of overpredictions based on ρ or s^{ex} that exceed 20% relative error correspond to the high density, low D state points near the freezing transition.
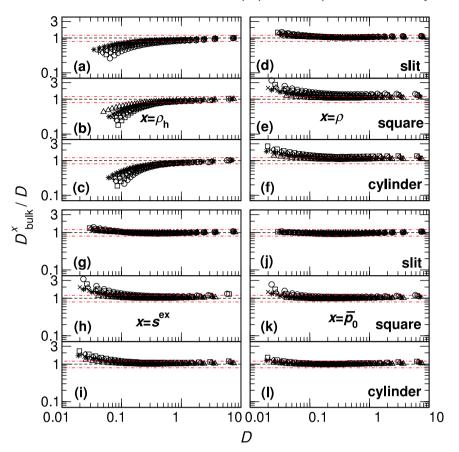
9

Figure 2. Ratio of self-diffusivity of a bulk HS fluid to that of a confined HS fluid with the same value of a static quantity x, D^x_{bulk}/D, obtained via molecular simulations. Data are shown for the fluid confined to slit pore ((a), (d), (g), (j)), square channel ((b), (e), (h), (k)), and cylindrical pore ((c), (f), (i), (l)) geometries. The static quantity x is indicated in each of the four panels. 20% bounds on relative error in confined fluid self-diffusivity 'predictions' obtained by using the bulk structure–property relation D^x_{bulk} are shown by red dash–dotted lines. The equilibrium fluid states shown here span the density range $0 < \rho_{\text{h}} < \rho_0$, where $\rho_0 \approx 0.95$ for ((a)–(c)) and $1 < \rho_0 < 1.25$ for ((d)–(l)), depending on pore size. Pores shown have confining dimensions of 5 ($\bigcirc$), 6 ($\square$), 7 ($\lozenge$), 8 ($+$), 9 ($\times$), 10 ($*$), and 15 ($\triangle$). These dimensions correspond to channel width H for slit pores and square channels and channel diameter d for cylindrical pores. All channels have smooth hard boundaries.

It might be tempting to conclude, on the basis of the slit pore data, that total-volume-based average density ρ tracks dynamics nearly as reliably as s^{ex} and $\overline{p_0}$ for confined fluids. To provide a more stringent test of this preliminary conclusion, we now examine D^x_{bulk}/D for HS fluids confined to quasi-one-dimensional square channel and cylindrical pore geometries with edge dimensions $H \geq 5$ and diameters $d \geq 6$, respectively. Fluids confined in these geometries have a significantly higher percentage of particles near the boundaries than in the corresponding slit pores, and hence the effects of confinement on both structure and dynamics should be more pronounced.

Figures 2(e) and (f) show that for square channel and cylindrical geometries, self-diffusivity predictions based on D_{bulk}^{ρ} can be significantly higher than the actual D of a confined fluid with the same ρ. In fact, for the densest fluid systems studied here, the bulk structure–property relation D_{bulk}^{ρ} is between 2 and 4 times larger than D, depending on H. Furthermore, figures 2(h), (i), (k) and (l) illustrate that D_{bulk}^{x} predictions for $x = s^{\text{ex}}$ or $x = \overline{p_0}$ are in the semi-quantitative range for a larger fraction of state points than those based on $x = \rho$. Specifically, D_{bulk}^{x} is within 20% of D for 46% ($x = \rho$), 82% ($x = s^{\text{ex}}$), and 95% ($x = \overline{p_0}$) of the state points. The main differences occur for high density, low D state points, where predictions based on fractional available volume are significantly more accurate than those based on excess entropy or density.

Another relevant test case for comparing which of ρ, s^{ex}, or $\overline{p_0}$ most faithfully tracks dynamics is to vary the degree of confinement while fixing ρ, an idea motivated by an earlier study by Mittal *et al* [3]. In particular, Mittal *et al* demonstrated that D and s^{ex} for a HS fluid oscillate in phase when H for the confining slit pore is varied (for $H \leq 5$) and ρ is held constant. The maxima in D (high particle mobility) and s^{ex} (weak interparticle correlations) occur for integer values of H, geometries which naturally accommodate the layering of particles near the boundaries. The minima in D (low particle mobility) and s^{ex} (strong interparticle correlations) occur for non-integer values of H, which frustrate this natural layering pattern. Along similar lines, Goel *et al* [9] recently demonstrated that particle–boundary interactions that flatten the density profile of a confined fluid generally reduce D and s^{ex}, while those which increase layering can have the opposite effect. All of this suggests that excess entropy captures some of the subtle frustration induced effects that layering has on both interparticle correlations and single-particle dynamics [3]. Does $\overline{p_0}$ also capture these effects? A very recent study of Mittal *et al* [10] suggests that it might. In particular, the authors of that study showed that the local fraction of available volume $p_0(z)$ and the position-dependent self-diffusivity normal to the boundaries $D_{\perp}(z)$ of a confined HS fluid are highest in regions of high local density $\rho(z)$.

Figure 3 provides a more direct test of this idea. In particular, it shows the D data of Mittal *et al* [3] for a HS fluid confined between hard walls calculated via molecular dynamics simulations. We have also included on this plot predictions from the three bulk structure–property relations D_{bulk}^{x}, where $x = \rho$, s^{ex}, and $\overline{p_0}$. Since ρ is fixed here, it is evident that D_{bulk}^{ρ} is not able to yield predictions of the oscillatory trends in the dynamics data. However, note that both $D_{\text{bulk}}^{s^{\text{ex}}}$ and $D_{\text{bulk}}^{\overline{p_0}}$ predict the correct oscillatory behavior. In fact, the predictions of $D_{\text{bulk}}^{\overline{p_0}}$ are virtually quantitative over the entire range of H.

Should we expect $D_{\text{bulk}}^{\overline{p_0}}$ to generally track the dynamics of dense, confined HS fluids more accurately than $D_{\text{bulk}}^{s^{\text{ex}}}$? In other words, what is more relevant for dynamics of inhomogeneous fluids: available space or available states? We further explore that question by examining the behavior of the confined HS mixture discussed in section 3. Specifically, by studying this binary fluid mixture in a slit pore with $H = 5$, we are able to probe confined fluid states with packing fraction ϕ as high as 0.52 (compared with the highest packing fraction of 0.46 for a monodisperse HS fluid confined in a slit pore of $H = 5$). At $\phi = 0.52$, the fluid already exhibits dynamic signatures of supercooling, e.g., the emergence of a plateau in the time dependence of the mean squared displacement. The corresponding D at this packing fraction (=0.002) is an order of magnitude smaller than the smallest D for the confined monodisperse fluid (=0.02) in the slit pore geometry.
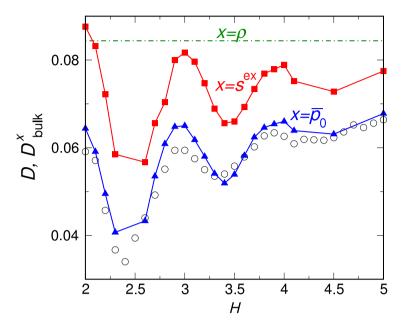
Figure 3. Self-diffusivity D of a HS fluid confined in narrow slit pores of width $H = 2$–5 by smooth hard boundaries. The density of the confined fluid is fixed at $\rho = (6/\pi)0.4$. We compare molecular dynamics simulation data (○) for the confined fluid with the self-diffusivity of a bulk HS fluid, D_{bulk}^x, at the same value of $x = \rho$ (green dash–dotted line), $x = s^{\text{ex}}$ (red square), and $x = \overline{p_0}$ (blue triangle). Solid lines are shown as a guide to the eye. D and s^{ex}, calculated via molecular dynamics and TMMC simulations, respectively, are taken from figure 7 of [3]. $\overline{p_0}$ was calculated via TMMC simulations described in section 3 of the present work.

Figures 4(a) and (b) show the ratio of the bulk self-diffusivity to confined self-diffusivity, D_{bulk}^x/D, for the small and large particles of the mixture, respectively. Again, the comparisons are made to the bulk fluid mixture of the same composition and density ($x = \rho$), excess entropy ($x = s^{\text{ex}}$), or fractional available volume of the corresponding species ($x = \overline{p_{0i}}$). Note that the bulk structure–property predictions for self-diffusivities of small and large particles are semi-quantitative (within 20%) for $D > 0.1$ when based on any of the three aforementioned static quantities. However, relative errors in predictions based on ρ or s^{ex} begin to increase sharply for $D < 0.1$. On the other hand, predictions based on $\overline{p_{0i}}$ remain semi-quantitative for all $D > 0.02$ (covering three decades in D), with significant overpredictions occurring only for the densest three state points investigated. Thus, it appears that, for single-particle dynamics, fractional available volume is the most relevant of the three static measures investigated here. The question of whether there exists an alternative static measure x such that D_{bulk}^x tracks D for deeply supercooled mixtures is currently an open one. The answer to that question will likely have important implications for understanding how confinement shifts the glass transition of fluids.

4.2. Particle–boundary interactions and a generalized measure of available volume

Thus far, we have only considered the geometric (i.e., packing) consequences of confinement on dynamics. How does the presence of finite particle–boundary interactions
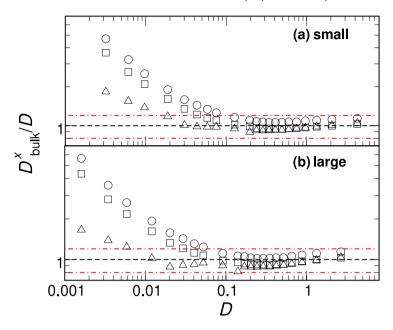
Figure 4. Ratio of self-diffusivity of (a) small particles and (b) large particles of a bulk binary HS fluid mixture to that of a corresponding confined HS fluid mixture with the same value of a static quantity x, D^x_{bulk}/D, obtained via molecular simulation. The static quantity used for making predictions is $x = \rho$ ($\bigcirc$), $x = s^{\mathrm{ex}}$ ($\square$), and $x = \overline{p_{0_i}}$ ($\triangle$). Data are shown for the $H = 5$ slit pore geometry with the total packing fraction in the range 0.025–0.52. The mole fraction of the small spheres is 0.75. 20% bounds on relative error in self-diffusivity predictions are shown by a red dash–dotted line.

affect the picture described in section 4.1? We explore the answer to this question by studying a monodisperse HS fluid confined to a slit pore geometry by smooth walls with either square shoulder (repulsive) or square well (attractive) particle–boundary interactions (for details, see equation (2)).

Figures 5(a) and (b) show the ratio of the bulk to confined self-diffusivity, D^x_{bulk}/D, for these two cases, respectively, with comparisons between bulk and confined fluids being made at the same density ($x = \rho$), excess entropy ($x = s^{\mathrm{ex}}$), and fractional available volume ($x = \overline{p_0}$). Clearly, the fractional available volume $\overline{p_0}$ fails to track the dynamics of the confined fluid for both cases presented. However, this should perhaps be expected. Since the interactions of the particles with the boundaries in these cases are strongly position dependent, all free space is not equally 'available' to the particles. To account for this energetic imbalance, we suggest a generalized available volume ($\overline{p_{0\mathrm{w}}}$) that appropriately weights the local available space with the Boltzmann factor of the particle–boundary interaction,

$$\overline{p_{0\mathrm{w}}} = \frac{\int_{V_c} p_0 \exp[-u_{\mathrm{w}}(s)]\,\mathrm{d}V}{\int_{V_c} \exp[-u_{\mathrm{w}}(s)]\,\mathrm{d}V} = \frac{\rho_{\mathrm{h}}(\xi)}{\rho_{\mathrm{h}}^{\mathrm{ig}}(\xi)} = \frac{\xi^{\mathrm{ig}}(\rho_{\mathrm{h}})}{\xi(\rho_{\mathrm{h}})} = \exp[-\{\mu(\rho_{\mathrm{h}}) - \mu^{\mathrm{ig}}(\rho_{\mathrm{h}})\}] \tag{6}$$

where, in all cases, the superscript 'ig' denotes the corresponding quantity for an ideal gas confined to an identical slit pore. As one can see from the above equation, since this generalized available volume inherently relates the thermodynamic state of the confined
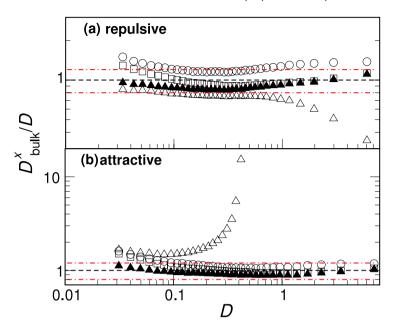
Figure 5. Ratio of self-diffusivity of a bulk HS fluid to that of a confined HS fluid with the same value of a static quantity x, D^x_{bulk}/D, obtained via molecular simulation. Data include systems with (a) square shoulder (repulsive) and (b) square well (attractive) particle–boundary interactions (see equation (2)) with $H = 5$ in the slit pore geometry. The static quantity used for making predictions is $x = \rho$ ($\bigcirc$), $x = s^{\text{ex}}$ ($\square$), $x = \overline{p_0}$ ($\triangle$), and $x = \overline{p_{0\text{w}}}$ ($\blacktriangle$). 20% bounds on relative error in self-diffusivity predictions are shown by the red dash–dotted line. Particle-center-accessible density for the fluid spans the range $0 < \rho_{\text{h}} < 1.05$. $\overline{p_0}$ overpredicts high diffusivity state points in panel (b) by more than 1000% and those data points are off the scale of the graph.

fluid to that of an ideal gas, it bears some resemblance to an excess thermodynamic property.

It is important to point out that this generalized available volume has several distinguishing features. (i) It reduces to $\overline{p_0}$ in the limit of fluids confined to smooth hard boundaries. Thus, all of the results presented earlier in this paper for $\overline{p_0}$ will remain unchanged for those systems if one instead uses $\overline{p_{0\text{w}}}$. (ii) Unlike the case for $\overline{p_0}$ or density, there is no arbitrary choice that needs to be made about the volume over which one should do the averaging. This quantity is the same no matter whether averaging is carried out over the center-accessible or the total volume of the fluid. Put differently, this definition removes any arbitrariness as regards the effective 'diameter' of the fluid–boundary interaction. (iii) The quantity $\overline{p_{0\text{w}}}$ can be computed directly from knowledge of standard thermodynamic and system parameters, namely ρ, ξ, and $u_{\text{w}}(z)$. (iv) It is not limited to HS fluid systems. In fact, the computation of $\overline{p_{0\text{w}}}$ from equation (6) does not even require information about the particle–particle interactions, as long as the other thermodynamic quantities can be measured.

How well does this new generalized measure of available volume track self-diffusivity when finite particle–boundary interactions are present? Figure 5 clearly illustrates that $\overline{p_{0\text{w}}}$ corrects for the problems that $\overline{p_0}$ faces in predicting the dynamics in these cases.

In particular, the maximum error in self-diffusivity predictions based on $\overline{p_{0\mathrm{w}}}$ is 16% across the entire range of packing fractions investigated, which makes it a more reliable predictor of single-particle dynamics than either s^{ex} or ρ for these systems. As was seen earlier, diffusivity predictions based on the bulk structure–property relation for $\overline{p_{0\mathrm{w}}}$ are considerably more accurate than that for ρ or s^{ex} when considering high density, low diffusivity state points ($D < 0.1$).

5. Using DFT together with bulk structure–property relations to predict dynamics of confined fluids

Above we have shown that knowledge of D_{bulk}^{x} for the bulk HS fluid ($x = s^{\mathrm{ex}}$ or $\overline{p_{0\mathrm{w}}}$) together with the value of x in confinement is enough for a semi-quantitative prediction of confined (equilibrium) fluid diffusivity, D, across a wide range of parameter space in these systems. Thus far, we have used TMMC simulations to determine x for each confined fluid of interest. That raises the following question. Is classical DFT accurate enough in its predictions of x that one can eliminate the step of simulating the confined fluid altogether? In this section, we take a first step toward addressing this question. In particular, we present calculations of the ratio of self-diffusivity of a bulk HS fluid to that of a confined HS fluid with the same value of x, D_{bulk}^{x}/D, where $x = s^{\mathrm{ex}}$ or $\overline{p_{0\mathrm{w}}}$. In each case, x for the confined fluid is obtained directly from predictions of Rosenfeld's fundamental measure theory [34, 35], an accurate DFT for these systems.

Figure 6 shows relative errors in self-diffusivity predictions based on s^{ex} and $\overline{p_{0\mathrm{w}}}$, comparing cases with knowledge of the 'exact' value of x in confinement (calculated via TMMC simulations) and the predicted value of x (calculated via DFT). Selected cases explored in section 4 involving the three confining geometries (slit pore, cylindrical pore, and square channel), small and large particles of binary mixtures, and finite fluid–boundary interactions are presented. In all cases, the D_{bulk}^{x}/D curves obtained via the two routes (TMMC versus DFT) are virtually indistinguishable over the entire density range of equilibrium fluid, a demonstration of the reliability of DFT for computing the static properties of these systems. As a result, it is clear that one can use the bulk structure–property relations discussed above together with predictions of x from DFT to make semi-quantitative estimates of confined fluid self-diffusivity for a wide variety of hard-sphere systems.

6. Conclusions

Fluids trapped in small spaces feature prominently in science and technology, and understanding their properties is key for a number of research areas that range from the design of membranes to the engineering of microfluidic devices. The static and dynamic properties of these confined fluids can be very different than those of bulk samples. While quantitatively accurate theories like DFT are available for predicting static properties of confined fluids, making even qualitative predictions for dynamics of inhomogeneous fluids has long been a challenging endeavor. In this paper, we demonstrate how semi-quantitative (albeit indirect) predictions of self-diffusivity are still possible, even in the absence of a theory, once one empirically recognizes that certain relationships between static and dynamic properties are insensitive to confinement.
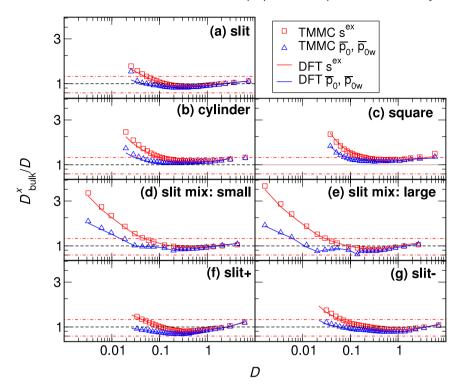
Figure 6. Ratio of self-diffusivity of a bulk HS fluid to that of a confined HS fluid with the same value of a static quantity x, D_{bulk}^x/D. Here we show a comparison of D_{bulk}^x/D with x obtained from the DFT (lines) or TMMC (symbols) calculations. ((a)–(c)) Data for a monodisperse HS fluid confined by smooth hard boundaries to a slit pore ($H = 5$), a cylindrical pore ($H = 6$), and a square channel ($H = 5$) geometry, respectively. ((d), (e)) Data for small and large particles of a binary HS mixture confined in an $H = 5$ slit pore, respectively. ((f), (g)) Data for a monodisperse HS fluid confined between the repulsive and attractive boundaries discussed in the text, respectively, placed at a separation of $H = 5$ in slit pore geometry. The density range for the state points shown are the same as in figure 2 for (a)–(c), figure 4 for (d) and (e), and figure 5 for (f) and (g). 20% bounds on relative error in self-diffusivity predictions are shown by the red dash–dotted line.

This study provides a systematic and quantitative investigation of such relationships. In particular, we present a comprehensive study of the effects of confinement on correlations between self-diffusivity (D) and various thermodynamic measures for confined HS fluids: particle-center-accessible-volume-based and total-volume-based average densities (ρ_h and ρ, respectively), excess entropy (s^{ex}), and two average measures of fractional available volume ($\overline{p_0}$ and $\overline{p_{0w}}$). Our main findings are as follows. The bulk structure–property correlation, D_{bulk}^x, based on the first density measure, $x = \rho_h$, severely underestimates D when ρ_h for the confined fluid is used as the input. Further, for dense confined fluids, ρ_h is often larger than the freezing density of the bulk fluid, eliminating altogether the possibility of using the corresponding bulk structure–property relation for predictions. Self-diffusivity predictions based on the relation with total-volume-based

density $x = \rho$ provide a significant improvement over those involving ρ_{h}, substantiating the earlier idea that ρ might be considered as a more natural measure of density for predicting dynamics [11].

However, when one considers a wider variety of geometries (slit pore, cylindrical, square channel), confined fluid mixtures, finite particle–boundary interactions, and a wide range of packing fractions, one finds that structure–property relations D^x_{bulk} based on excess entropy ($x = s^{\mathrm{ex}}$) and a new generalized measure of available volume ($x = \overline{p_{0\mathrm{w}}}$) provide much more accurate estimates for D than those based on either of ρ_{h} or ρ. Importantly, neither $\overline{p_{0\mathrm{w}}}$ nor s^{ex} requires one to arbitrarily define an averaging volume for the confined system.

We note that predictions about how confinement modifies self-diffusivity based on $\overline{p_{0\mathrm{w}}}$ become significantly more accurate than those based on s^{ex} under conditions of very high packing fractions (e.g., supercooled fluids) and highly restrictive confining geometries (e.g., quasi-one-dimensional channels). The generalized available volume $\overline{p_{0\mathrm{w}}}$ may also be easier to compute on the basis of experimental quantities than s^{ex}, since the former is related to average density and chemical potential in a simple way (see equation (6)). In the limit of hard spheres confined between hard walls, $\overline{p_{0\mathrm{w}}}$ reduces to the fraction of available volume p_0, which is a purely geometric quantity. Interestingly, a recent experimental study has demonstrated that p_0 can be measured in hard-sphere colloidal suspensions using confocal microscopy [39]. Single-particle dynamics in these systems can also be readily measured [26]. Hence, confined colloidal suspensions appear to represent a promising class of experimental systems for testing the generality of the results presented here.

Predictions of static properties (x) via classical DFT are sufficiently accurate for inhomogeneous HS fluids that one can use them, together with the bulk structure–property relation (D^x_{bulk}), to make semi-quantitative estimates of confined fluid diffusivities. This heuristic approach effectively eliminates the need for simulating the confined fluid altogether, which might be particularly convenient in applications where one needs to estimate the dynamics of systems across a wide array of parameter space. For example, in the design of microfluidic systems, one might hope to screen a large range of possible particle–boundary interactions or confining geometries against design considerations. A preliminary application of this idea [9] is to use DFT to passively tune the transport properties of a confined fluid, in a controlled way, by modifying the geometry or boundary–particle interactions of the confined space.

Can the aforementioned static measures yield predictions of the dynamics of fluids with continuous intermolecular potentials and/or attractive interactions? As mentioned earlier, recent data from molecular simulations have shown that there is indeed an isothermal correlation between the self-diffusion coefficient D and the excess entropy for a variety of confined fluids (e.g., Lennard-Jones, square well, Weeks–Chandler–Andersen ones [40]), approximately independent of the degree of confinement for a wide range of equilibrium conditions [9, 12]. We are currently exploring the viability of using the generalized available volume for predicting dynamics in these fluids, and we will report on our findings in a future study.

In terms of other related future directions, we are now beginning to study how well using the static properties examined in this work we can forecast changes in other transport properties of fluids (i.e., viscosity and thermal conductivity) under confinement. We are also studying how aspects of the (static) solvation shell structure surrounding large

tracer particles relate to their single-particle dynamics. Results of these studies will be explored in detail in future publications.

Acknowledgments

References

[1] Davis H T, *Kinetic theory of inhomogeneous fluid: tracer diffusion*, 1987 *J. Chem. Phys.* **86** 1474
[2] Vanderlick T K and Davis H T, *Self-diffusion in fluids in microporous solids*, 1987 *J. Chem. Phys.* **87** 1791
[3] Mittal J, Errington J R and Truskett T M, *Does confining the hard-sphere fluid between hard walls change its average properties?*, 2007 *J. Chem. Phys.* **126** 244708
[4] Happel J and Brenner H, 1973 *Low Reynolds Number Hydrodynamics* (Dordrecht: Kluwer)
[5] Faucheux L P and Libchaber A J, *Confined brownian motion*, 1994 *Phys. Rev.* E **49** 5158
[6] Lin b, Yu J and Rice S A, *Direct measurements of constrained brownian motion of an isolated sphere between two walls*, 2000 *Phys. Rev.* E **62** 3909
[7] Dufresne E R, Altman D and Grier D G, *Brownian dynamics of a sphere between parallel walls*, 2001 *Europhys. Lett.* **53** 264
[8] Saugey A, Joly L, Ybert C, Barrat J L and Bocquet L, *Diffusion in pores and its dependence on boundary conditions*, 2005 *J. Phys.: Condens. Matter* **17** S4075
[9] Goel G, Krekelberg W P, Errington J R and Truskett T M, *Tuning density profiles and mobility of inhomogeneous fluids*, 2008 *Phys. Rev. Lett.* **100** 106001
[10] Mittal J, Truskett T M, Errington J R and Hummer G, *Layering and position-dependent diffusive dynamics of confined fluids*, 2008 *Phys. Rev. Lett.* **100** 145901
[11] Mittal J, Errington J R and Truskett T M, *Thermodynamics predicts how confinement modifies the dynamics of the equilibrium hard-sphere fluid*, 2006 *Phys. Rev. Lett.* **96** 177804
[12] Mittal J, Errington J R and Truskett T M, *Relationships between self-diffusivity, packing fraction, and excess entropy in simple bulk and confined fluids*, 2007 *J. Phys. Chem.* B **111** 10054
[13] Mittal J, Shen V K, Errington J R and Truskett T M, *Confinement, entropy, and single-particle dynamics of equilibrium hard-sphere mixtures*, 2007 *J. Chem. Phys.* **127** 154513
[14] Truskett T M, Torquato S and Debenedetti P G, *Towards a quantification of disorder in materials: distinguishing equilibrium and glassy sphere packings*, 2000 *Phys. Rev.* E **62** 993
[15] Mittal J, Errington J R and Truskett T M, *Quantitative link between single-particle dynamics and static structure of supercooled liquids*, 2006 *J. Phys. Chem.* B **110** 18147
[16] Errington J R, Truskett T M and Mittal J, *Excess-entropy-based anomalies for a waterlike fluid*, 2006 *J. Chem. Phys.* **125** 244502
[17] Krekelberg W P, Mittal J, Ganesan V and Truskett T M, *How short-range attractions impact the structural order, self-diffusivity, and viscosity of a fluid*, 2007 *J. Chem. Phys.* **127** 044502
[18] Mittal J, Krekelberg W P, Errington J R and Truskett T M, *Computing free volume, structural order, and entropy of liquids and glasses*, 2007 *Reviews in Computational Chemistry* vol 25, ed K B Lipkowitz and T R Cundari (New York: Wiley–VCH) pp 125–58
[19] Rosenfeld Y, *Relation between the transport coefficients and the internal entropy of simple systems*, 1977 *Phys. Rev.* A **15** 2545
[20] Rosenfeld Y, *A quasi-universal scaling law for atomic transport in simple fluids*, 1999 *J. Phys.: Condens. Matter* **11** 5415
[21] Dzugutov M, *A universal scaling law for atomic diffusion in condensed matter*, 1996 *Nature* **381** 137
[22] Widom B, *Some topics in the theory of fluids*, 1963 *J. Chem. Phys.* **39** 2808

[23] Lebowitz J L, Helfand E and Praestgaard E, *Scaled particle theory of fluid mixtures*, 1965 *J. Chem. Phys.* **43** 774
[24] Widom B, *Structure of interfaces from uniformity of the chemical potential*, 1978 *J. Stat. Phys.* **19** 563
[25] Henderson J R, *Statistical mechanics of fluids at spherical structureless walls*, 1983 *Mol. Phys.* **50** 741
[26] Nugent C R, Edmond K V, Patel H N and Weeks E R, *Colloidal glass transition observed in confinement*, 2007 *Phys. Rev. Lett.* **99** 025702
[27] Rapaport D C, 2004 *The Art of Molecular Dynamics Simulation* (Cambridge: Cambridge University Press)
[28] Errington J R, *Direct calculation of liquid–vapor phase equilibria from transition matrix Monte Carlo simulation*, 2003 *J. Chem. Phys.* **118** 9915
[29] Shen V K and Errington J R, *Determination of fluid-phase behavior using transition-matrix Monte Carlo: binary Lennard-Jones mixtures*, 2005 *J. Chem. Phys.* **122** 064508
[30] Ferrenberg A M and Swendsen R H, *New Monte Carlo technique for studying phase transitions*, 1988 *Phys. Rev. Lett.* **61** 2635
[31] Carnahan N F and Starling K E, *Equation of state for nonattracting rigid spheres*, 1969 *J. Chem. Phys.* **51** 635
[32] Boublík T, *Hard-sphere equation of state*, 1970 *J. Chem. Phys.* **53** 471
[33] Mansoori G A, Carnahan N F, Starling K E and Leland T W Jr, *Equilibrium thermodynamic properties of the mixture of hard spheres*, 1971 *J. Chem. Phys.* **54** 1523
[34] Yu Y and Wu J, *Structures of hard-sphere fluids from a modified fundamental-measure theory*, 2002 *J. Chem. Phys.* **117** 10156
[35] Roth R, Evans R, Lang A and Kahl G, *Fundamental measure theory for hard-sphere mixtures revisited: the white bear version*, 2002 *J. Phys.: Condens. Matter* **14** 12063
[36] Rosenfeld Y, *Free-energy model for the inhomogeneous hard-sphere fluid mixture and density-functional theory of freezing*, 1989 *Phys. Rev. Lett.* **63** 980
[37] Gonzalez A, White J A, Roman F L and Velasco S, *Density functional theory of fluids in nanopores: analysis of the fundamental measures theory in extreme dimensional-crossover situations*, 2006 *J. Chem. Phys.* **125** 064703
[38] Sears M P and Frink L J D, *A new efficient method for density functional theory calculations of inhomogeneous fluids*, 2003 *J. Comput. Phys.* **190** 184
[39] Dullens R P A, Aarts D G A L and Kegel W K, *Direct measurement of the free energy by optical microscopy*, 2006 *Proc. Nat. Acad. Sci.* **103** 529
[40] Chandler D, Weeks J D and Andersen H C, *van der Waals picture of liquids, solids, and phase transformations*, 1983 *Science* **220** 787